$O(2)$ symmetry constrained mode interactions in 2D cylinder wake flow

N.W. Mureithi*

Department of Mechanical Engineering, École Polytechnique, Box 6079, Station Centre-ville, Montréal, QC, H3C 3A7, Canada

Abstract

A fundamental symmetry group theoretic analysis of the periodically forced cylinder wake dynamics problem is presented. The analysis yields a clear and concise explanation of experimentally observed cylinder wake dynamics.

First it is shown that the underlying problem can be posed as a mode interaction problem subject to $O(2)$ symmetry constraints. An analysis of the amplitude equations for **S**/**K** mode interactions predicts the experimentally observed period-doubling instabilities when $\lambda_s/\lambda_k = 1/1$. For 2/1 wavelength ratio, it is shown that traveling wave solutions are to be expected. Furthermore, the apparent lack of interactions for 3/1 ratio is shown to be due to the fact that important nonlinear coupling terms appear only at 7th order.

For asymmetrical **K1**/**K** mode interactions, the symmetry 'compatibility', via common subgroups, explains the strong resonances observed experimentally for 1/1 and 1/3 frequency ratios. For a frequency ratio 1/2, it is shown that **K1** and **K** mode symmetries are incompatible. Consequently, traveling wave solutions most likely underlie the organized wake topology observed in experiments.

Keywords: Karman wake; Mode interactions; Bifurcations; Symmetry group; Normal forms

1. Introduction

The present study follows a body of work by various investigators, e.g. Ongoren et al. [1], Williams et al. [2], Krishnamoorthy et al. [3], Mureithi et al. [4] and Mureithi [5]. The goal of these studies is to uncover the underlying dynamic properties of the Karman wake. External excitation is introduced at frequencies (ω) forming rational ratios with the natural shedding Karman frequency, (Ω). Symmetry arguments have been used by Williams et al. for instance to explain the lack of lock-in for certain frequency ratios (ω/Ω). Recently Mureithi et al. [4] and Mureithi [5] have formalized this relation to symmetry by deriving general amplitude equations for general Karman wake symmetrical or asymmetrical excitation.

* Tel.: +1 (514) 340 4711; Fax: +1 (514) 340 4176; E-mail: Njuki.mureithi@polymtl.ca

Computational Fluid and Solid Mechanics 2005
K.J. Bathe (Editor)

2. Amplitude equations and mode interactions

2.1. Flow symmetry

The flow field behind the cylinder may be expressed (approximately) in terms of a finite number of dominant wake modes (patterns). The Karman shedding mode is designated **K**. A second well known mode is the reflection symmetric shedding mode **S**. Assuming that all other modes (besides modes **S**,**K**) are stable, the x-direction velocity perturbations, for instance, may be expressed as

$$u(x,y,t) = S(t)\,\Psi_S(y)e^{i(\lambda_S x+\omega_s t)} + K(t)\,\Psi_K(y)e^{i(\lambda_K x+\omega_K t)} + \text{complex conjugate} \quad (1)$$

where $S(t)$ and $K(t)$ are the mode amplitudes for mode **S** and **K**, respectively, and λ_s, λ_k the corresponding wave numbers. For the Karman mode **K**, the modal symmetry may be compactly expressed as

$$\Gamma_K = Z_2(\kappa,\pi) \times S^1 \quad (2)$$

Γ_s and Γ_k must be subgroups of the base symmetry Γ. The symmetry Z_2 (κ, π) is a combined spatial-temporal symmetry. The 'circular' symmetry S^1 pertains to the (local) periodicity in the flow associated with the Hopf bifurcations which marks the onset of vortex shedding. The mode **S** symmetry may be compactly expressed by

$$\Gamma_S = D_m(\kappa, \frac{2\pi}{m}) \times S^1 \tag{3}$$

2.2. Amplitude equations

Consider the following system of ODEs:

$$dx/dt = g(x), \quad x \in R^n, \quad g : R^n \to R^n \tag{4}$$

The invertible matrix $\gamma \in R^{nxn}$ is called a ***symmetry*** of $g(x)$ if $\gamma g(x) = g(\gamma x)$, $\forall x \in R^n$. The function $g(x)$ is also referred to as a γ -equivariant function. Given a symmetry group Γ, it can be shown that there exists a finite set of basis functions (Γ-equivariant polynomials) that generates the complete set of Γ-equivariant functions; proof of this is given by the Hilbert-Weyl (HW) theorem [6]. The amplitude equations governing mode interactions between modes **S** and **K**, having wavelength ratio $\lambda_k/\lambda_s = m/n$, can be derived based on the Hilbert-Weyl theorem. The final result, derived by Mureithi et al. [4], takes the following form for the interaction functions (when m is odd):

$$\begin{bmatrix} \Phi_S \\ \Phi_K \end{bmatrix} = \begin{bmatrix} p(r_1,r_2,r_3)S + q(r_1,r_2,r_3)\bar{S}^{n-1}K^m \\ r(r_1,r_2,r_3)K + s(r_1,r_2,r_3)S^n\bar{K}^{m-1} \end{bmatrix} \tag{5}$$

In Eq. (5), the 'coefficients' p, q, r, s are polynomial functions of the Γ-invariant functions $r_1 = S\bar{S}$, $r_2 = K\bar{K}$, $r_3 = S^n\bar{K}^m$, $\bar{r}_3 = \bar{S}^nK^m$ and the wavelength ratio $\lambda_k/\lambda_s = m / n$ with m and n relatively prime. The **S** mode equation, for instance, in discrete form is, $S_{n+1} = \Phi_s(S_n, K_n)$.

2.3. Mode interaction dynamics

2.3.1. 1/1 mode interaction

For the case $\lambda_K/\lambda_S = m/n = 1$ the amplitude equations in polar form are

$$\begin{aligned} r_{n+1} &= \left(1 + \alpha_0 + \alpha_2 r_n^2 + \gamma_{11} q_n^2\right) r_n + \delta_{01} q_n^2 r_n \cos 2\theta_n \\ q_{n+1} &= \left(1 + \beta_0 + \beta_2 q_n^2 + \gamma_{21} r_n^2\right) q_n + \mu_{01} q_n r_n^2 \cos 2\theta_n \\ \theta_{n+1} &= \theta_n - q_n r_n (\mu_{01} r_n + \delta_{01} q_n) \sin 2\theta_n \end{aligned} \tag{6}$$

where $K = re^{i\phi}$, $S = qe^{i\Psi}$ and $\theta_n = \Psi_n - \phi_n$.

Several conclusions can be drawn from the form of Eq. (6). Steady-state solutions are obtained for $\cos 2\theta = \pm 1$. Traveling wave solutions occur when $\mu_{01} r_n + \delta_{01} q_n = 0$ with $\sin 2\theta_n \neq 0$.

A bifurcation analysis of the map (6) by Mureithi et al. [4] showed that a period-doubling instability of the **K** mode is induced by **S**-mode excitation (forcing). The period-doubling instability is demonstrated in the CFD computations of Fig 1. The computations were performed at Re = 1918. The **S** mode is 'generated' by forced cylinder oscillations at a frequency ω parallel to the upstream flow. The shedding frequency behind the stationary cylinder is Ω. For all the dynamic simulations presented in what follows, the cylinder was oscillated with an amplitude of 0.3D.

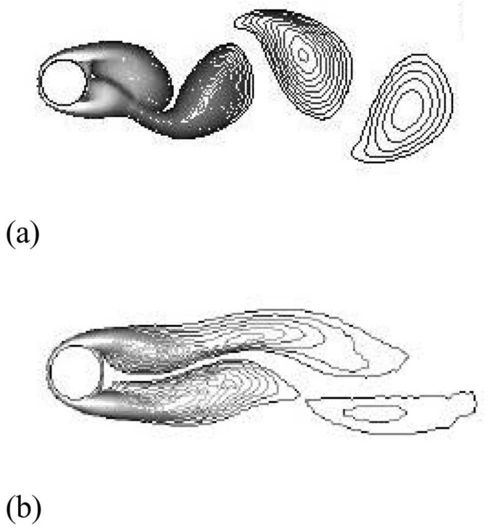

Fig. 1. Wake vortex for (a) stationary cylinder (a) compared to an oscillating cylinder (b), with $\omega/gV = 1$.

2.3.2. 2/1 mode interaction

For $\lambda_K/\lambda_S = m/n = 2$ the amplitude equations in polar form are

$$\begin{aligned} r_{n+1} &= \left(1 + \alpha_0 + \alpha_2 r_n^2 + \bar{\gamma}_{11} q_n^2\right) r_n + \bar{\delta}_{01} q_n r_n \cos \theta_n \\ q_{n+1} &= \left(1 + \bar{\beta}_0 + \bar{\beta}_2 q_n^2 + \bar{\gamma}_{21} r_n^2\right) q_n + \bar{\mu}_{01} r_n^2 \cos \theta_n \\ \theta_{n+1} &= \theta_n - \frac{1}{q_n}(\bar{\mu}_{01} r_n^2 + 2\bar{\delta}_{01} q_n^2) \sin \theta_n \end{aligned} \tag{7}$$

where $\theta_n = \Psi_n - 2\phi_n$. Steady-state (SS) solutions correspond to fixed points of the map (7) when $\cos\theta = \pm 1$. For $\cos\theta_n \neq \pm 1$, the fixed points correspond to traveling wave (TW) solutions. Further details on the solutions and their stabilities may be found in Porter et al. [7]. A numerical simulation result for this wavelength ratio is shown in Fig. 2(b) where comparison is made with the case of a stationary cylinder shown in Fig. 2(a). Unlike the case $\lambda_k/\lambda_s = 1$ discussed above, no period doubling instability occurs. The snapshot of the wake in Fig. 2(b) looks strikingly similar to the stationary cylinder wake. Closer inspection reveals that the reflection symmetry of the **S** mode is broken via merging of two vortices for each forcing cycle. Based on the description of possible solutions above, the most likely candidate for the solution of Fig. 2(b) is the traveling wave (TW) solution. The traveling nature of the solution is a direct consequence of the $Z_2(\kappa)$ symmetry breaking of the **S** mode. An inspection of the map (7) shows that the existence of a pure **K** mode solution requires the rather non-generic condition that $\bar{\mu}_{01} = 0$. A pure **S** mode solution although allowed by the map (10) does not correspond to the vortex pattern seen in Fig. 2(b).

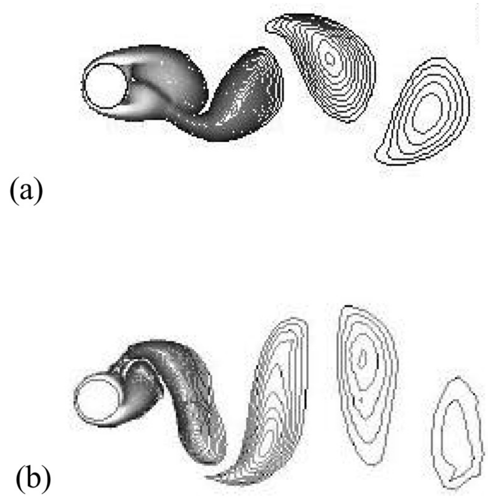

Fig. 2. Wake vortex for (a) fixed cylinder (a) compared to a moving cylinder (b), with $\omega/\Omega = 2$.

2.3.3. 3/1 mode interaction

For $\lambda_k/\lambda_s = m/n = 3$ the amplitude equations in polar form become

$$
\begin{aligned}
r_{n+1} &= (1 + \alpha_0 + \alpha_2 r_n^2 + \bar{\bar{\gamma}}_1 q_n^2) r_n + \bar{\bar{\delta}}_{01} q_n^2 r_n^5 \cos 2\theta_n \\
q_{n+1} &= (1 + \bar{\bar{\beta}}_0 + \bar{\bar{\beta}}_2 q_n^2 + \bar{\bar{\gamma}}_{21} r_n^2) q_n + \bar{\bar{\mu}}_{01} q_n r_n^6 \cos 2\theta_n \\
\theta_{n+1} &= \theta_n - q_n r_n^5 (3\bar{\bar{\delta}}_{01} q_n + \bar{\bar{\mu}}_{01} r_n) \sin 2\theta_n
\end{aligned}
\tag{8}
$$

The map (8) shows important coupling only at 7th order between the modes for this wavelength ratio. This prediction is borne out by the numerical simulations results shown in Fig. 3. The vortex structures for two instantaneous cylinder positions, equilibrium and maximum (0.3D) downstream displacement are respectively shown in Figs. 3(a) and 3(b). One-and-half shedding cycles downstream, the wake has completely recovered the regular Karman structure.

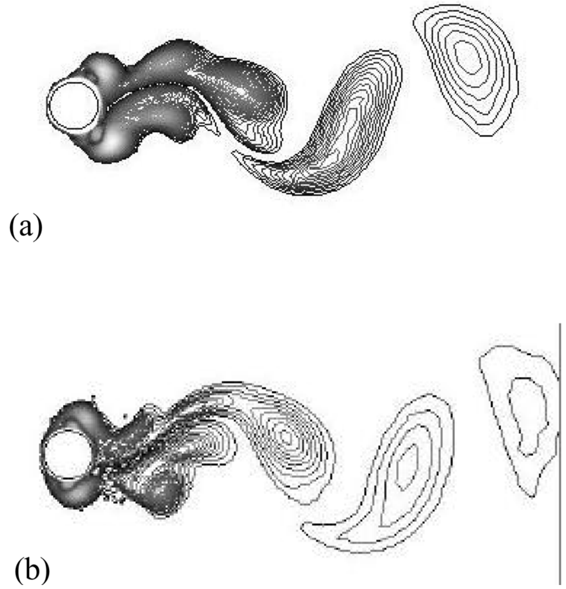

Fig. 3. Wake vortex for a moving cylinder with $\omega/\Omega = 3$ and cylinder position (a) 0.0D and (b) 0.3D downstream from equilibrium.

2.4. **K1/K** *mode interaction dynamics*

In this section, we highlight the important findings regarding **K1/K** mode interactions. The **K1** mode has Z_2 $(\kappa, n\pi)$. For harmonic/subharmonic ($\omega/\Omega = 1/1, 1/2, 1/3$) excitation, significant lock-ins (resonances) can be expected. The relationships between the **K1** and **K** mode symmetries are shown in the partial isotropy lattices of Fig. 4 for $\omega/\Omega = 1/2$ and $1/3$.

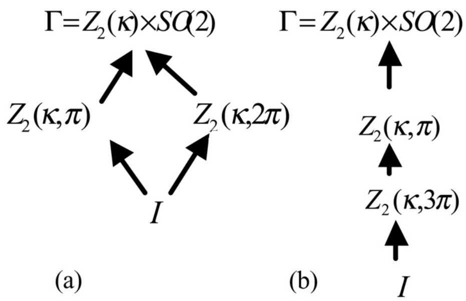

Fig. 4. Symmetry isotropy lattice for cross-flow excitation with (a) $\omega/\Omega = 1/2$ and (b) $\omega/\Omega = 1/3$, respectively.

Since the symmetry Z_2 (κ,3π) is common to both **K1** and **K** modes, strong mode (steady state) interaction can be expected for $\omega/\Omega = 1/3$. For $\omega/\Omega = 1/2$ the **K1** and **K** modes have no common symmetries. Consequently, interaction between the modes cannot result in a steady state solution. Although symmetry limitations do not allow steady state mode locking, unsteady solutions corresponding to traveling waves are allowed. Expressing the complex amplitudes in the polar forms $K_n = k_n e^{i\psi_n}$, $F_n = f_n e^{i\phi_n}$, the mode interaction mapping in this case is

$$\begin{aligned} k_{n+1} &= (1 + \alpha_0 + \alpha_{12} f_n^2 + \alpha_2 k_n^2) k_n + \beta_0 k_n f_n^4 Cos\Theta_n \\ f_{n+1} &= (1 + \gamma_0 + \gamma_{12} f_n^2 + \gamma_2 k_n^2) f_n + \delta_0 k_n^2 f_n^3 Cos\Theta_n \\ \Theta_{n+1} &= \Theta_n - 4 k_n f_n^3 (\delta_0 k_n + \tfrac{1}{2}\beta_0 f_n) Sin\Theta_n \end{aligned} \tag{9}$$

where $\Theta_n = 2(2\phi_n - \psi_n)$. A traveling wave solution is obtained when $(\delta_0 k_n + \frac{1}{2}\beta_0 \mathrm{f_n}) = 0$. Returning to the experimental results reported in the literature, it is clear that an organized wake structure will be observed and that depending on the speed of the traveling wave, the structure may appear quasi-stationary.

3. Concluding remarks

The general form of the wake mode amplitude equations has been presented and qualitatively analyzed. The **S/K** mode interaction equations are found to predict the experimentally observed period-doubling instabilities when $\lambda_s/\lambda_k = 1/1$, while traveling waves may be expected for 2/1 wavelength ratio. Lack of low-order coupling for 3/1 ratio points to the lack of significant mode interaction observed in experiments and confirmed numerically.

For asymmetrical **K1/K** mode interactions, a basic symmetry group analysis conclusively shows that no mode-lockin should be expected for 1/2 wavelength ratio, rather, traveling wave solutions should underly the organized wake topology seen in experiments.

References

[1] Ongoren A, Rockwell D. Flow structure from an oscillating cylinder, part 1 and 2. J Fluid Mech 1988;191:197–245.

[2] Williams DR, Mansy H, Amato C. The response and symmetry properties of a cylinder wake subjected to localized surface excitation. J Fluid Mech 1992;234:71–96.

[3] Krishnamoorthy S, Price SJ, Paidoussis MP. Cross-flow past an oscillating circular cylinder: synchronization phenomena in the near wake. J Fluids Struct 2001;15:955–980.

[4] Mureithi NW, Kanki H, Goda S, Nakamura T, Kashikura T. Symmetry breaking and mode interaction in vortex-structure interaction. In: Proc of the 5th International Symposium on FSI, AE and FIV + N, ASME International Mechanical Engineering Congress and Exhibition, New Orleans, Louisiana, USA. Paper IMECE 2002–32512, 2002.

[5] Mureithi NW. Implications of symmetry in inline and Karman shedding mode interaction. NAGARE J Jap Soc Fluid Mech 2003;22:211–227.

[6] Golubitsky M, Stewart I, Schaeffer DG. Singularities and Groups in Bifurcation Theory, Vol. II. New York: Springer, 1988.

[7] Porter J, Knoblock E. New type of complex dynamics in the 1:2 spatial resonance. Physica D 2001;159:125–154.